AIAA-99-3588

Supersonic Coaxial Jet Experiment for CFD Code Validation

A.D. Cutler, A.A. Carty and S.E. Doerner
The George Washington University, JIAFS,
Hampton, VA

G.S. Diskin and J.P. Drummond
NASA Langley Research Center, Hampton, VA

30th AIAA Fluid Dynamics Conference
28 June - 1 July, 1999/Norfolk, VA

AIAA-99-3588

SUPERSONIC COAXIAL JET EXPERIMENT FOR CFD CODE VALIDATION

A. D. Cutler*, A. A. Carty†, S. E. Doerner‡
The George Washington University, JIAFS, Hampton, VA
G. S. Diskin§, J. P. Drummond¶
*NASA Langley Research Center, Hampton, VA***

ABSTRACT

A supersonic coaxial jet facility has been designed to provide experimental data suitable for the validation of CFD codes used to analyze high-speed propulsion flows. The center jet is of a light gas and the coflow jet is of air, and the mixing layer between them is compressible. Various methods have been employed in characterizing the jet flow field, including schlieren visualization, pitot, total temperature and gas sampling probe surveying, and RELIEF velocimetry. A Navier-Stokes code has been used to calculate the nozzle flow field and the results compared to the experiment.

INTRODUCTION

There is a need for data sets to validate computational fluid dynamics (CFD) codes used to analyze high-speed propulsion flows, such as those in supersonic combustion ramjets (scramjets). Such data sets should have well-defined inlet conditions and flow geometries, and flow fields that have been well documented using a variety of instrumentation. These data sets should also provide a challenging and relevant test of the codes, particularly the empirically-based turbulence models.

Previous detailed experimental studies of high speed mixing flows have tended to either concentrate on the simplest case of a two-stream planar mixing layer or on the much more complex problems of injection and mixing (and enhancement of mixing) in a supersonic duct flow. There now exists a large body of work on the two-stream planar mixing layer. Many of these are phenomenological studies intended to gain understanding of the effects of compressibility on mixing - Dimotakis[1] reviews much of this literature. Some of the cases studied may have been sufficiently well documented for code validation. However, high-speed propulsion flows tend to have only relatively small regions which resemble the two stream planar mixing layer, while in the greater part of an engine mixing occurs between partially mixed fuel-air plumes and "free-stream" air (there being no "core" of unmixed fuel remaining). A number of well documented studies of injection into a supersonic duct flow exist (e.g., Donohue and McDaniel[2]) and these provide excellent test cases, representative of scramjet flows [3]. However, such flows are very complex and there is need for detailed data sets in a flow of intermediate complexity.

The geometry chosen for the experiment was that of a coaxial jet discharging into stagnant laboratory air, with center jet of a light gas (a mixture of 5% oxygen and 95% helium by volume) and coflow jet of air. Both coflow and center-jet nozzles were operated to provide exit flow at 1 atmosphere. The presence of oxygen in the center-jet gas was to allow the use of an oxygen flow-tagging technique (RELIEF[4]) to obtain non-intrusive velocity measurements in the flow. Both jets are nominally Mach 1.8, but because of the greater speed of sound of the center-jet gas the velocity in the

---

*Associate Professor, Senior Member AIAA

†Graduate Research Scholar Assistant, Member AIAA, now at Lockheed Martin Corp., Palmdale, Ca.

‡Graduate Research Scholar Assistant, Member AIAA, now at Raytheon Corp. Tucson, Az.

§Research Scientist, Senior Member AIAA

¶Senior Research Scientist, AIAA Associate Fellow

center jet is more than twice that of the coflow jet. The two stream mixing layer which forms between the center jet and the coflow near the nozzle exit is compressible, with an average of the calculated convective Mach number[5] of the center jet relative to the mixing layer and that of the mixing layer relative to the coflow, M_c, of 0.7.

Table 1 gives various parameters of the experiment. From top to bottom these are: gas molecular weight and ratio of specific heats, Mach number, assumed total temperature, nozzle exit velocity, exit static pressure, exit pitot pressure, and pressure at the center jet reference plane. Pressures are non-dimensionalized by the pressure at the coflow reference plane. From left to right, the columns refer to the coflow, the center jet if the center-jet gas is air, and the center jet if the center-jet gas is helium-oxygen. These parameters (except for gas properties and total temperature) were calculated assuming isentropic flow of a calorically perfect gas and one-dimensionality at the upstream (low speed) reference plane, the throat and the exit of each (center jet and coflow) nozzle. Upstream reference, throat, and exit areas were specified.

The coaxial jet geometry has several advantages: It includes both a two stream mixing layer (between center-jet gas and coflow air) near the nozzle exit and a plume of center-jet-gas/air mixture downstream of the point where the core of pure center-jet gas ends. Since it is a free jet, it provides easy access for both optical instrumentation and probes. Because it is axisymmetric, it requires a minimum number of experimental measurements to fully characterize, and CFD calculations of it can be performed with relatively modest computer resources. However, a disadvantage of an axisymmetric geometry is that shock waves strengthen as they approach the axis, and turn normal on the axis itself, complicating the flow in this region. Care was thus taken in the design of the facility to provide as near as possible to 1-D flow at the exit of both center and coflow nozzles, and to minimize the strength of waves generated at the nozzle exit.

Previous studies of coaxial jets[6,7,8] were studies of the effects of convective Mach number and of the relative mixing performance of circular, rectangular and elliptical center jets. These were not efforts to obtain data suitable for code validation.

FLOW FACILITY

The coaxial jet assembly is shown in Fig. 1. It is axisymmetric and consists of an outer body and a center body. The space between these bodies forms the coflow jet nozzle, and the interior passage of the center body forms the center-jet nozzle. The details of this facility have been described by Carty[9].

The center body was manufactured in two pieces. The tip, containing the convergent-divergent part of the center-jet nozzle was machined separately and furnace brazed to the longer upstream part. The center body is locked into a concentric ring by a nut, and this ring in turn is supported by three streamlined struts located in the low speed part of the coflow nozzle. Flow entering the center body is made uniform and of low turbulence by five screens compressed between copper washers whose internal diameter matches that of the center body downstream.

The outer body consists of four parts: At the top, a conical extension ring, which is normally in place, but can be removed to provide optical or probe axis to the flow at the center-jet nozzle exit. Below that the contoured section of the outer body, followed by the section containing the center body support struts, and finally a mating flange. Note that sharp corners were provided at the entrance to the coflow nozzle, both at the mating flange and at the start of the center body. The resulting separations should ensure turbulent boundary layers, thereby providing a known transition location for flow calculations and reducing or eliminating any (non-axisymmetric) separations at the center body support strut junctions.

The nozzle assembly is joined to the Transverse Jet Facility, located in the laboratories of the Hypersonic Airbreathing Propulsion Branch at NASA Langley Research Center. The plenum of this facility includes acoustic dampening and flow conditioning screens. Center-jet gas is provided to the center body through the mating flange. Air is provided to the facility from a central air station, and the helium-oxygen mixture is provided from a bottle trailer containing premixed gas.

The assembly is instrumented with pressure taps: one in the center body just downstream of the screens, one in the coflow nozzle plenum, and one in the outer body near the exit of the coflow nozzle (in a region where the flow has reached its exit condition). Thermocouples were located in the gas supply lines to

measure temperature, and ambient (barometric) pressure was also read. The values of these various quantities during the probe surveys are given in Table 2 for the three test cases. Note that tabulated uncertainties are due to facility unsteadiness and variations in set point, and are found by taking 2× the root mean square variations during the tests. They do not include ±0.5% in pressures and ±2 K in temperatures due to transducer error. Facility unsteadiness and variations in set point are less than the transducer error for pressures and pressure ratios. However, since air and helium-oxygen supply temperature could not be controlled, variations in temperatures and temperature ratios are higher.

The facility was designed for helium-oxygen in the center jet but some flow field data were also acquired for two other cases: First, with no flow in the center jet, producing a jet with a wake on its axis and a complex shock system. Second, with air in the center jet (at nominal 1 atmosphere exit pressure), producing a coaxial jet flow with very little velocity difference between the center jet and coflow but influenced by the boundary layers which develop on the center body and the wake of the lip. This data, obtained with no helium-oxygen expenditure and relatively little extra effort, could be used for additional validation cases.

NOZZLE CONTOURS

The following procedure was employed in designing the "inviscid" contour of both center jet and coflow nozzles:

The surface contour in the subsonic region of the nozzle was specified by patching together smooth curves in such a way that second derivatives were continuous. Numerical solution of the Euler equations was performed to establish surface pressure distributions, and contour geometry was iterated upon to ensure no significant surface pressure drop in the region of concave curvature at the beginning of the contraction. This precaution was to avoid the possibility of boundary layer separation.

The throat and supersonic initial expansion contour region was specified by means of a smooth function with zero second derivative at the downstream end of the initial expansion region. Since the second derivative of the "turning contour" function (the wave cancellation surface of the nozzle) is zero at its upstream end and is continuous downstream, this ensures that second derivatives are continuous throughout the nozzle. The initial expansion region contours were iterated upon to provide an exit Mach number of 1.8. The flow in the supersonic region was calculated by the method of characteristics (MOC), with the turning contour specified to produce 1-D flow at the nozzle exit. Flow conditions along the initial value line for the MOC calculation were obtained using Sauer's transonic small perturbation method[10]. The coflow nozzle is unusual in that expansion occurs on the center body - the outer contour of this nozzle is parallel to the axis. This required that a MOC code be written especially for this work, and that Sauer's analysis (as presented by Zucrow and Hoffman[10]) be extended to account for the presence of the center body.

After design of the inviscid contours as described, the nozzle boundary layers were calculated using two different boundary layer codes[11,12] assuming first laminar, then turbulent flow, and, in the case of the Wilcox[12] code, utilizing both the Cebeci-Smith and k-ω turbulence models. Small discrepancies existed between the results from the different codes (as expected) but these were not significant. The method by which the final contours were obtained is illustrated in Fig. 2. The inviscid contours were corrected for the boundary layer by shifting them radially (toward larger flow area) by the displacement thickness obtained from the *turbulent* boundary layer calculations. Then, the coflow contour was truncated at the downstream end, and finally, the exit and axes of the center jet and coflow nozzles were aligned at x=0. The truncation was performed to avoid insufficient center-body wall thickness, i.e., insufficient distance between the center-jet and coflow nozzle contours. It also slightly reduced the thickness of the boundary layer at the end of the coflow nozzle surface. Figure 2 also shows the location of the limiting characteristic separating regions with M=1.8 and regions where M<1.8, based on the MOC calculation. The Mach number on the coflow center-body inviscid contour at x=0 is 1.742.

Errors were made during the computation of the final center-jet nozzle contour: After correcting for displacement thickness, the exit diameter of the center-jet nozzle contour was 5.12 mm rather than the target 5.00 mm. It was intended that both x and r dimensions of the nozzles simply be rescaled to correct for this. However, due to a miscommunication between two of the authors, only the radial dimension was rescaled. Additionally, it was subsequently discovered during the

experiment that this boundary layer was in fact laminar rather than turbulent as had been assumed. The effects of these errors will be discussed below.

As a check on the nozzle designs, and to provide input conditions for future calculations of the jet flow, the nozzle flows were calculated using the axisymmetric version of the SPARK Navier-Stokes code[13,14]. The flow in each nozzle was calculated using a grid starting at x=-246.4 mm and ending at x=0. The grid was 201×51 for the center-jet nozzle and 201×101 for the coflow nozzle. The coflow nozzle was also calculated with a 201×201, but the results changed negligibly, indicate adequate resolution. The grids were compressed in y near the walls, and were compressed in x in the vicinity of the throat and in the supersonic flow region. The boundary layer in the center-jet nozzle was assumed to be laminar and the boundary layers in the coflow nozzle were assumed to be turbulent. The Cebeci-Smith model[12] was employed. These assumptions of boundary layer state provided the best agreement between calculated and measure pitot pressure distributions at the nozzle exit (these measurements will discussed later).

Figure 3 shows contours of Mach number in the vicinity of the nozzle exit computed by the SPARK code. The M=1.79 contour may be compared to the limiting characteristic shown in Fig. 2. Note also the boundary layers, which are significant in thickness approaching the exit of the coflow nozzle. Figure 4 shows a plot of Mach number at the exit plane. Mach number is very close to 1.80 in the region where it is expected to be, i.e., downstream of the limiting characteristic. It is a little higher (≈1.82) at the exit of the center-jet nozzle, probably due to the previously discussed errors in design. In fact, this figure shows that the consequences of these errors are small, amounting to a slight change in Mach number.

FLOW FIELD MEASUREMENTS

Various types of flow field measurement have been performed:

SCHLIEREN

The flow has been visualized with conventional schlieren and shadowgraph. The system employed a 1 mm pulsed arc lamp of duration about 1 μsec, two 9 inch diameter 50 inch focal length achromat lenses, a razor blade mounted on a 3-axis positioner as a knife edge, and a digital camera with a CCD array, 18.4 mm×27.6 mm in size with 2000×3000 pixels, and a 135 mm focal length lens.

PROBES

Pitot, gas sampling, and total temperature probes, shown in Fig. 5, have been employed to survey the flow. The pitot probe is cylindrical and square tipped. The gas sampling probe internal passage diverges conically downstream of the tip, with probe and tubing internal diameters sized to avoid choking the sample gas flow, thereby ensuring shock attachment at the probe tip. The total temperature probe is a miniature shrouded, vented thermocouple. The probe incorporated a commercial microminiature thermocouple probe, the thermocouple junction of which was located at the tip of a 0.20 mm diameter "needle". The probes are mounted in a diamond-airfoil strut, and translated in the flow by a two component stepping-motor driven translation stage.

The gas flow acquired by the sampling probe is passed through coils in an ice bath and roughly 90% of it is then vented to the atmosphere at low speed. The remaining roughly 10% is drawn over a fiber-film probe connected to a hot-wire anemometer bridge circuit, and then through a choked orifice. The sampled gas passing over the hot film is at 0°C and, because of the discharge to the atmosphere, is at atmospheric pressure (independent of the total flow rate). Thus, the fiber-film probe response is dependent only upon gas composition. The system is calibrated regularly by flowing known mixtures of helium-oxygen and air and fitting bridge output voltage to a 4th order polynomial function. The calibration mixtures are provided by mixing flows of helium-oxygen and air provided by digital mass flow controllers. Calibrations are checked prior and subsequent to testing to ensure calibration drift is less than about ±0.3% in mole fraction. The largest contribution to the uncertainty of the system is due to the manufacturer-quoted ±1% of full scale in the mass flow controller used for controlling the helium-oxygen calibration flow. Maximum uncertainty in mole fraction of helium-oxygen is in the range ±1-1.5%, but uncertainty is less than this close to mole fractions of 0.0 or 1.0 where uncertainty in the composition of the calibration mixture approaches zero. The technique is described in greater detail by Cutler and Johnson[15].

RELIEF

The RELIEF[4] (Raman Excitation plus Laser-Induced Electronic Fluorescence) oxygen flow tagging technique, illustrated in Fig. 6, has been used to provide measurements of (instantaneous) axial component velocity. RELIEF is a time-of-flight technique which involves two steps. In the first ("tag") step, oxygen in a line segment of the flow is excited to a non-equilibrium vibrational state by stimulated Raman scattering. This is achieved by focusing (50 cm focal length) collinear laser beams at 532nm and 580 nm. These beams are generated by passing a 200 mJ doubled Nd:YAG laser beam (532 nm) through a 6.9 MPa Raman cell containing a 50:50 mixture of helium and oxygen. The Raman cell is seeded with light from a broadband dye laser pumped by doubled residual infrared light from the Nd:YAG laser. The non-equilibrium oxygen returns to equilibrium only slowly as it convects with the flow. In the second "probe" step of the technique, the non-equilibrium region is found by laser-induced fluorescence imaging. This is achieved with a 20 mJ narrow band (approximately 0.5 cm^{-1}) ArF excimer (193 nm) laser beam cylindrically focused to a 10 mm high ×0.5 mm thick sheet in the region where the tagged flow is expected to be. The resulting fluorescence is imaged using a double intensified video-rate CCD camera, with f/4.5 UV lens and extension rings for closeup operation. Data were acquired at 5 Hz.

The resulting data consist of images of displaced line pairs, acquired either at different delay times after the tag, or with one of the lines acquired prior to operation of the jet (i.e., with zero flow velocity). The instantaneous velocity is determined by finding, in subsequent data reduction, the line displacement at various points along it, and dividing by the probe delay time. A calibration is required to establish the relationship between position in the image and position in space. Mean u-component velocity and root mean square fluctuation can be obtained by the technique. This work is currently in progress, and only limited preliminary data were taken. Uncertainties in this data are probably less than ±3%.

RESULTS

Figure 7 shows a typical schlieren result with vertical knife edge and nozzle conical extension ring removed. Vertical dark and bright stripes may be seen at the left and right edge respectively of the center jet, and also at the right and left edge of the coflow jet, due to large transverse gradients of refractive index. Notice also the shock/expansion wave structure emanating outward from the (0.25 mm thick) center body lip. Similar shocks propagate inward into the center jet, but are not visible in the schlieren due to the low refractive index within the center jet. The continuation of these initially inward propagating shocks, after they have crossed at the axis and passed out of the center jet into the coflow air, are visible.

Figure 8 shows a comparison between the measured pitot pressure at x=0.13 mm and pitot pressure derived from the CFD calculation at x=0. (Pitot pressure was obtained from the CFD result by computing the total pressure downstream of a normal shock at each grid point, assuming isentropic flow of a calorically perfect gas.) Agreement is good in the coflow, but the pitot data seem to scatter (in a symmetrical fashion) above and below the calculation in the center jet. This is believed to be neither error in the measurements (these features are very repeatable) nor computational error, but rather, due to small manufacturing errors (differences between the specified and actual nozzle contours) in the center-jet nozzle. Difficulties were encountered in manufacturing the center-jet nozzle due to the small size and inaccessability of the surface. In retrospect, and based on experience in manufacturing even smaller convergent-divergent nozzles, a better result could have been obtained using electrical-discharge machining. Figure 9 shows a comparison between the measured pitot pressure in the vicinity of the nozzle lip and the results of boundary layer calculations performed with the Wilcox code[12]. It may be seen that conventional turbulence modeling of the boundary layers gives good results. It should be noted that the pitot probe dimensions are not small in relation to the scale of this plot. Thus, the probe reads in error in the regions of steep pitot pressure gradient.

Figure 10 shows a comparison between RELIEF data at x=4.6 mm and the SPARK code calculation of the flow at x=0. There are some differences between the calculation and the data, which occur because of the difference in streamwise location. Waves (also observed in the schlieren) emanate from the lip at y=±5.0-5.25 mm, both towards the axis and away from it, and these influence the region of flow between ±1.5

and ±8.5 mm. For example, the RELIEF data shows a symmetrical pair of positive spikes in the center jet due to a conical expansion wave, and (less visible) matching negative spikes at slightly larger radius due to a (concentric) shock. Agreement between calculation and data inside ±1.5 mm and outside ±8.5 mm is excellent.

Figure 11 shows pitot pressure data in the jet. Plots are offset in the vertical direction by a distance 0.02× the x location (in mm) of the survey. The previously noted waves emanating from the center body lip are clearly visible in this data. For example, at x=10 mm the center jet has a symmetric pair of positive pitot pressure spikes due to the initially inward propagating waves from the lip, slightly downstream of the point where they cross the axis. The next 5-6 pitot surveys downstream of x=10 mm show a small negative spike at the axis. This is attributed to a defect in total pressure created by the inward propagating shock wave from the lip, which becomes stronger and forms a normal shock at the axis. Moving further downstream, the growing region of mixed air and helium-oxygen is seen as a region of pitot pressure deficit. The deficit is in part attributed to the initial deficit in total pressure due to boundary layers and the drag at the lip, and in part is attributed to continuing entropy rises due to the process of mixing. The data also reveal the growth of the coaxial jet into the ambient air.

Two pitot surveys with air as the center-jet gas acquired along the same diameter, 8 months apart, and a third along an othogonal diameter, all at x=100 mm, were identical within the uncertainty. (No figure is shown.) This confirmed that the data were repeatable and the flow axisymmetric.

Figure 12 shows the surveys of mole fraction of center-jet gas. The data are smooth and symmetrical, and show the radial growth of the mixing layer and plume. The radial location of 0.01 and 0.99 mole fraction was interpolated from the data for each survey, and the results are plotted as a function of x in Fig. 13. Also shown are curve fits to the data. The growth rate of the mixing layer between center jet and coflow, upstream of the point at x=150 mm where the inner boundary of the mixing layer intersects the axis, is 0.0333+0.0321=0.0654. The ratio of this experimental growth rate to the rate of growth of an incompressible mixing layer between streams of equal velocity and density ratios, computed as described by Papamoschou and Roshko[5], is 0.43. Compare this to the value 0.38, obtained from the following curve fit by Dimotakis[1] to experimental growth rate data from mostly two-dimensional planar mixing layers, and obtained by various techniques, including schlieren imaging, and pitot surveys:

$$\delta'/\delta_i' = 0.2 + 0.8\exp(-3M_c^2)$$

The difference between the present value and the value from the equation is not significant given the spread in the data fit by Dimotakis.

Figure 14 compares a probe survey of total temperature at x=100.25 mm with the simultaneously measured center jet supply temperature, both normalized with coflow air supply temperature. In the coflow the probe indicates a total temperature 0.99 of the coflow supply total temperature (it is usual for probes of this type to read slightly low). Close to the axis, where a small region of pure helium-oxygen still exists, the probe again reads about 1% low. However, in the mixing layer between center jet and coflow, there are small positive (+2%) and negative (-1%) excursions in total temperature, rather than a monotonic variation between the two limits. These deviations are believed to be real, but are small enough that it was not considered to be worthwhile to survey elsewhere in the jet with this probe.

CONCLUSIONS

A supersonic coaxial jet facility has been designed to produce data suitable for the validation of computational fluid dynamics codes. The nozzle geometries and flow inlet conditions have been adequately documented. Calculations of the flow in the nozzle using an axisymmetric Navier-Stokes code have been presented. Flow field measurements have been acquired at the nozzle exit plane and in the jet downstream using several techniques. These include schlieren imaging, gas sampling, pitot pressure and total temperature surveying, and RELIEF velocimetry. Agreements between experiment and calculations at the nozzle exit plane are good.

This research is continuing, with more extensive RELIEF velocimetry data being acquired, including not only mean u component velocity but also root mean square fluctuations. Calculations of the jet flow field, using both Reynolds-averaged Navier-Stokes equation and large eddy simulation methods, have just started.

The purpose of these calculations is to test various turbulence models used in the methods.

The George Washington University authors would like to acknowledge the support of NASA Langley Research Center through grant NCC-1-217.

REFERENCES

1.Dimotakis, P.E., "Turbulent Free Shear Layer Mixing and Combustion," in Murthy, S.N.B., Currran E.T. (eds.), *High-Speed Flight Propulsion Systems*, AIAA Progress in Astronautics and Aeronautics Series, Vol. 137, Washington DC, pp.265-340, 1991.

2.Donohue, J.M., and McDaniel J.C., "Complete 3-D Multi-Parameter Mapping of the Supersonic Mixing Flow field of a Ramp Fuel Injector," AIAA Paper 95-0519, 33rd Aerospace Sciences Meeting, Reno, NV, Jan. 9-12, 1995.

3.Eklund, D. R., Northam, G. B., and Fletcher, D. G., "A Validation Study of the SPARK Code for Nonreacting Scramjet Combustor Flowfields," AIAA Paper 90-2360, July 1990.

4.Diskin, G. S., "Experimental and Theoretical Investigation of the Physical Processes Important to the RELIEF Flow Tagging Diagnostic," Ph.D. Dissertation, Princeton University, 1997.

5.Papamoschou, D., Roshko, A., "The compressible turbulent shear layer: an experimental study," *J. Fluid Mech.*, vol 197, pp. 453-577, 1988.

6.Gutmark, E., Schadow, K.C., Wilson. K. J., "Effect of convective Mach number on mixing of coaxial circular and rectangular jets," *Phys. Fluids A.*, Vol. 3, No. 1, pp. 29-36, 1991.

7.Gutmark, E., Schadow, K.C., Wilson. K. J., "Mixing Enhancement in Coaxial Supersonic Jets," AIAA Paper 89-1812, AIAA 20th Fluid Dynamics, Plasma Dynamics and Lasers Conference, Buffalo NY, June 12-14, 1989.

8.Schadow, K.C., Gutmark, E., Wilson. K. J., "Passive Mixing Control in Supersonic Coaxial Jets at Different Convective Mach Numbers," AIAA paper 89-0995, AIAA 2nd Shear Flow Conference, Tempe, AZ, March 13-16, 1989.

9.Carty, A.A., "Development and Validation of a Supersonic Helium-Air Coannular Jet Facility," M.S. Thesis, The George Washington University, School of Engineering and Applied Sciences, August 1998.

10.Zucrow, M. J., Hoffman, J. D., *Gas Dynamics - Vol II - Multidimensional Flow*, pp. 87-103, Krieger, 1985.

11.Harris, J. E., Blanchard, D. K., "Computer Program for Solving Laminar, Transitional, or Turbulent Compressible Boundary-Layer Equations for Two-Dimensional and Axisymmetric Flow," NASA TM 83207, 1982.

12.Wilcox, D. C., *Turbulence Modeling for CFD*, 2nd Edition, Appendix C, DCW Industries, 1998.

13.Drummond, J. P., "A Two-Dimensional Numerical Simulation of a Supersonic, Chemically Reacting Mixing Layer," NASA TM 4055, 1988.

14.Carpenter, M. H., "Three-Dimensional Computations of Cross-Flow Injection and Combustion in a Supersonic Flow," AIAA Paper 89-1870, June 1989.

15.Cutler, A. D., Johnson, C. H., "Analysis of intermittency and probe data in a supersonic flow with injection," *Experiments in Fluids*, Vol. 23, pp. 38-47, 1997.

TABLES

Table 1 Calculated flow parameters assuming 1-D flow at low speed reference plane, throat and exit.

	Coflow	Centerjet	
Gas	Air	Air	5%O_2 + 95%He
MW	28.97	28.97	5.403
γ	1.4	1.4	1.645
M	1.8	1.721	1.8
T_t (K)	300	300	300
u_{exit} (m/s)	487	474	1097
$p_{exit}/p_{ref,coflow}$	0.1740	0.1740	0.1740
$p_{pit}/p_{ref,coflow}$	0.813	0.751	0.903
$p_{ref,CJ}/p_{ref,coflow}$		0.870	1.056

Table 2 Experimental flow parameters.

	Centerjet		
	None	Air	5% O_2 + 95% He
$p_{ref,coflow}$ (kPa)	580±2	580±2	580±2
$T_{t,coflow}$ (K)	299±6	300±6	300±6
$p_{ref,CJ}/p_{ref,coflow}$		0.873± 0.003	1.060± 0.008
$T_{t,CJ}/T_{t,coflow}$		0.976± 0.018	1.02±0.05
$p_{amb}/p_{ref,coflow}$	0.1759± 0.0010	0.1759± 0.0012	0.1758± 0.0012
$T_{amb}/T_{t,coflow}$	0.986± 0.018	0.983± 0.018	0.982± 0.017
$p_{exit}/p_{ref,coflow}$	0.1748± 0.0005	0.1748± 0.0005	0.1748± 0.0005

FIGURES

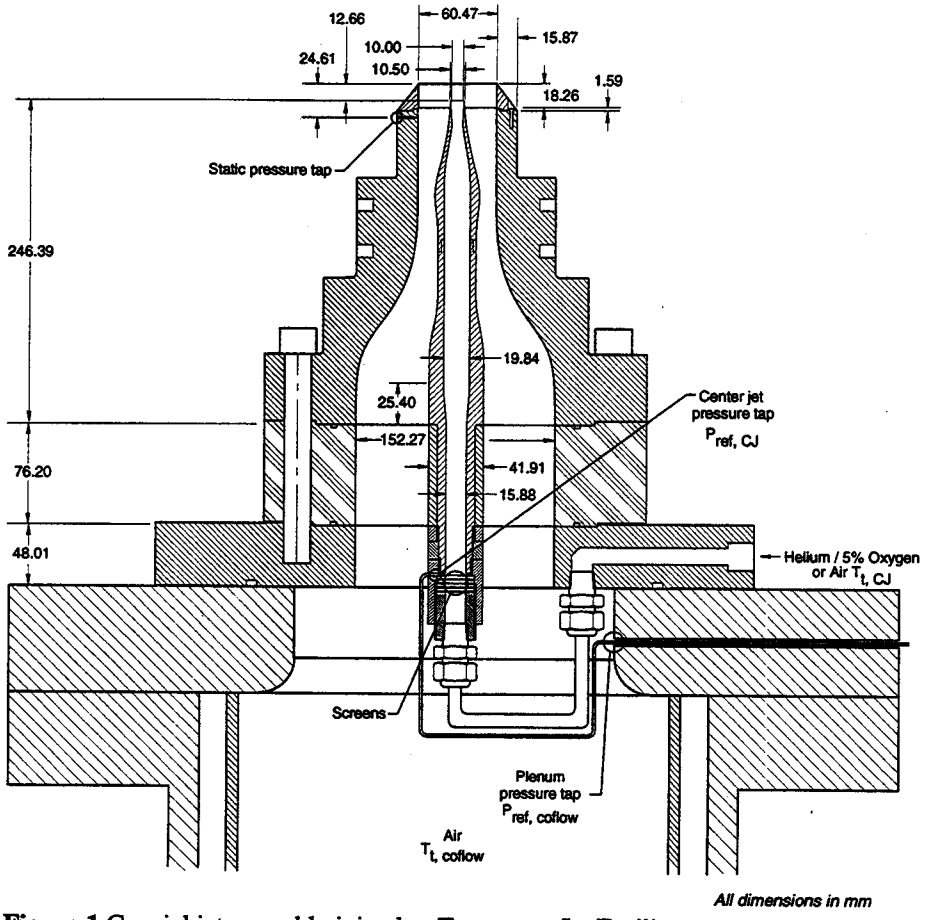

Figure 1 Coaxial jet assembly joined to Transverse Jet Facility.

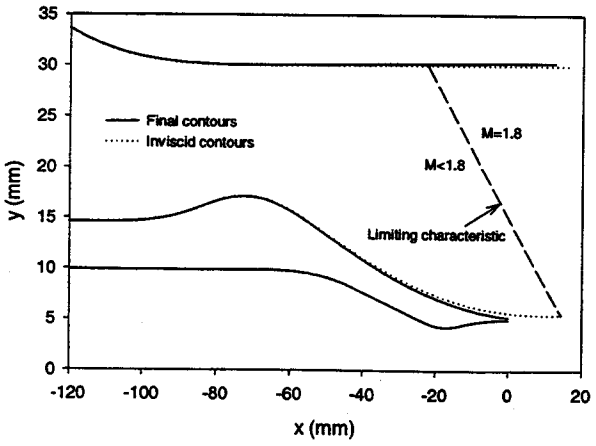

Figure 2 Method of characteristics and final geometry near nozzle exit.

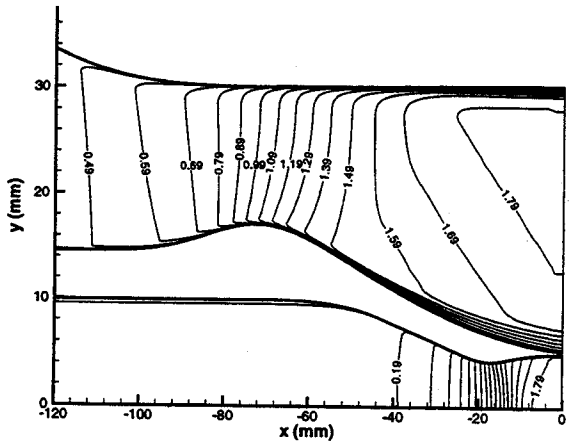

Figure 3 SPARK code calculation of Mach number.

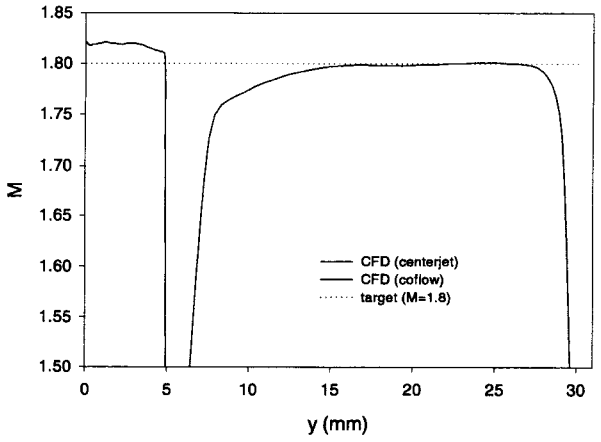

Figure 4 Calculated exit Mach number.

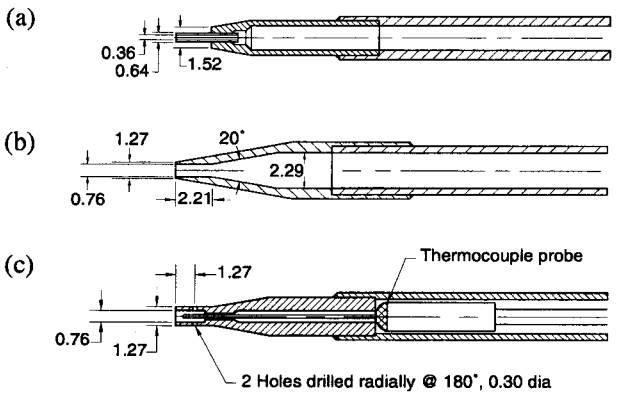

Figure 5 Probes: (a) pitot, (b) gas sampling, (c) total temperature.

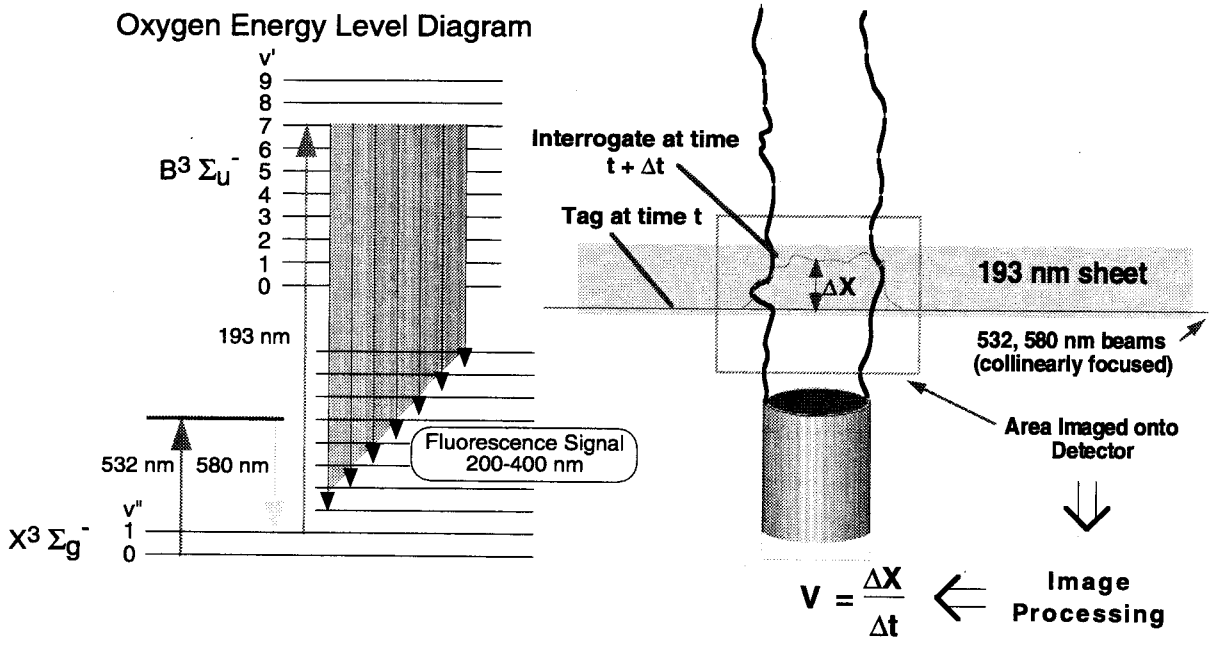

Figure 6 Schematic of RELIEF system.

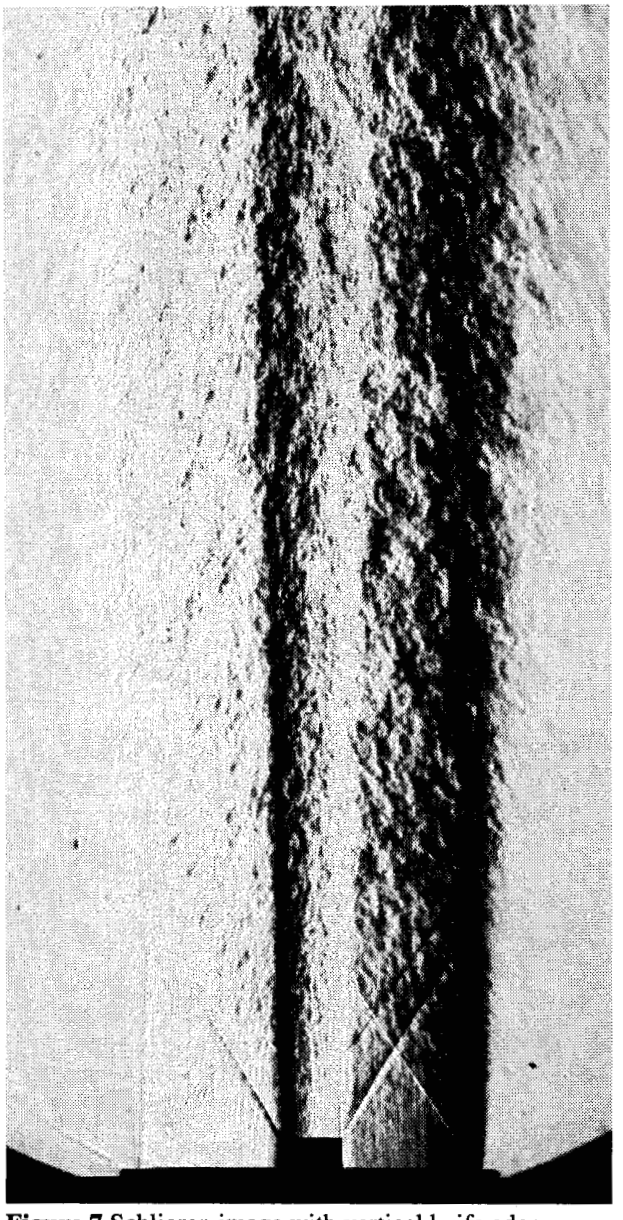

Figure 7 Schlieren image with vertical knife edge (conical extension cap removed)

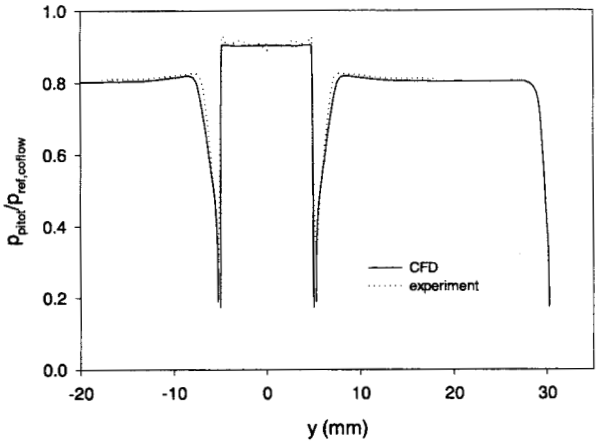

Figure 8 Comparison between pitot pressure data and SPARK code calculation at x=0.

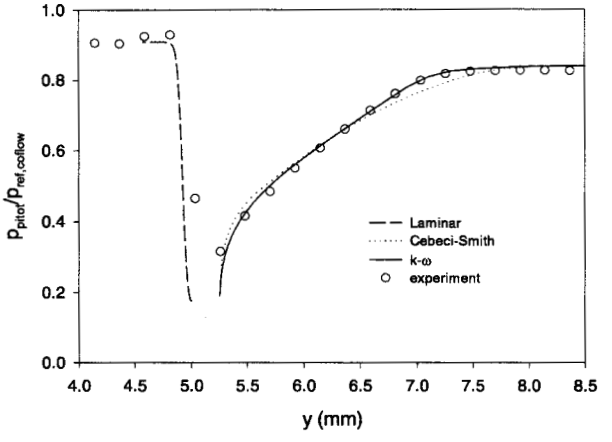

Figure 9 Comparison between pitot pressure data and boundary layer calculations at x=0.

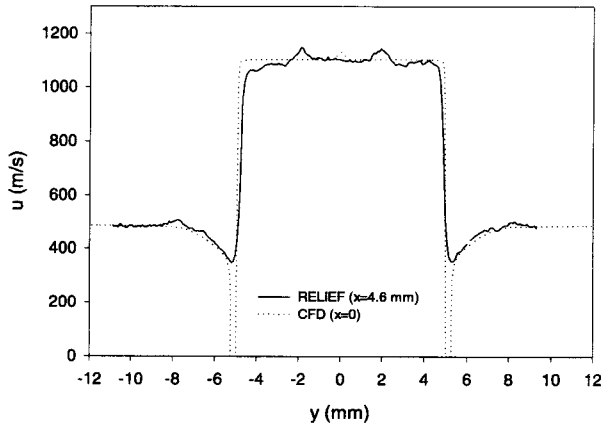

Figure 10 Comparison between preliminary RELIEF data and SPARK code calculation.

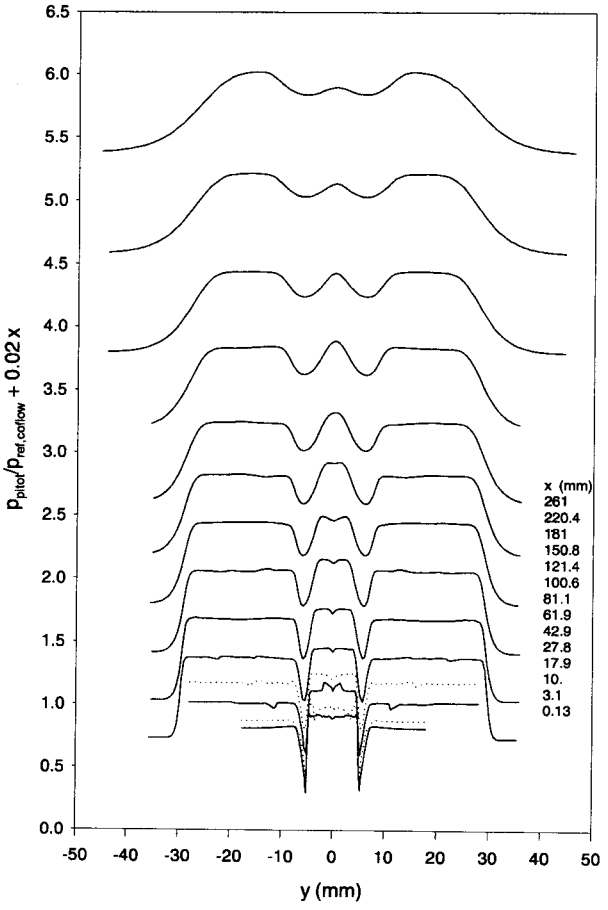

Figure 11 Pitot pressure surveys (note data are shifted up by 0.02 × the axial location).

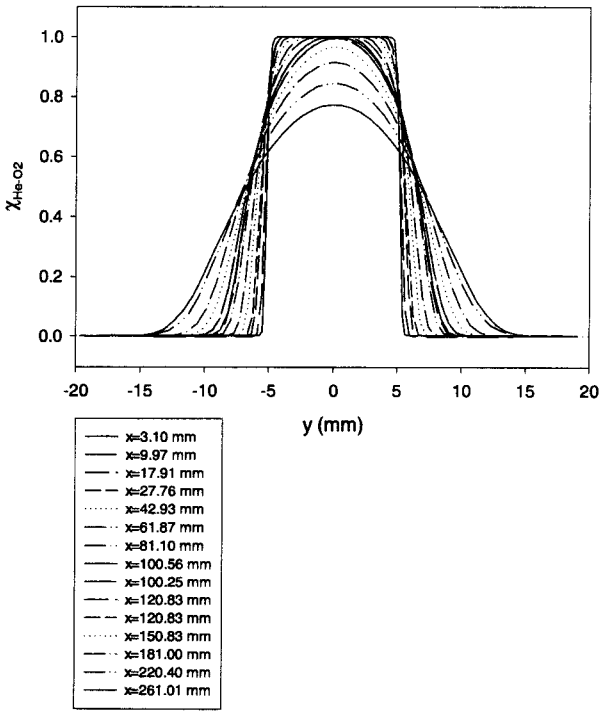

Figure 12 Mole fraction surveys.

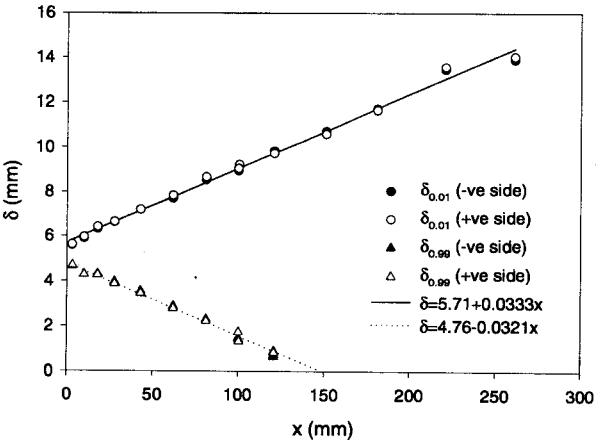

Figure 13 Mixing region (1% and 99% mole fraction He-O_2) boundaries.

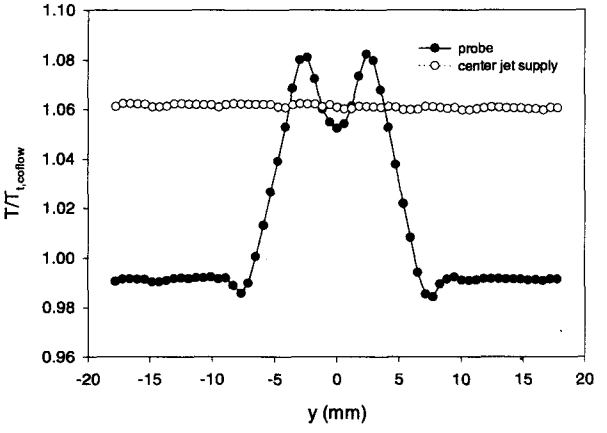

Figure 14 Total temperature distribution at x=100.25 mm and simultaneous center jet supply gas temperature.